
000 001 002 003 004 005 006 007 008 009 010 011 012 013 014 015 016 017 018 019 020 021 022 023 024 025 026 027 028 029 030 031 032 033 034 035 036 037 038 039 040 041 042 043 044 045 046 047 048 049 050 051 052 053 054 Emergent Biological Realism in RL-Trained DNA Language Models

Anonymous Authors¹

Abstract

Plasmids are essential DNA molecules widely used in research and biomanufacturing, yet their design remains complex and iterative. We introduce Plasmid-RL, a reinforcement learning framework for DNA language models that generates structurally valid and functionally coherent plasmid sequences. Using Group Relative Policy Optimization with a reward function based on synthetic biological constraints, our model achieves 97% quality control pass rate compared to 6% for the pretrained baseline. Remarkably, beyond explicitly optimized features, the model exhibits emergent biological parallels: generated sequences match natural plasmids in thermodynamic stability, codon usage patterns, and ORF length distributions, properties not directly encoded in the reward function. These results suggest that RL training steers the model toward biologically coherent regions of sequence space, analogous to how evolutionary optimization produces conserved functional patterns across diverse organisms.

1. Introduction

Plasmids are extrachromosomal DNA sequences, often found in bacteria, capable of replication independent of a host genome (Lederberg, 1952). These genetic elements are ubiquitous in biotechnology, serving as the primary vectors for protein expression, gene editing, and emerging DNA therapeutics (Kutzler & Weiner, 2008; Prather et al., 2003). Despite their widespread utility, plasmid engineering remains a complex, high-dimensional optimization problem. Traditional workflows are cost intensive and heuristic driven, often requiring iterative cycles of manual sequence editing and experimental validation to resolve structural instabilities (Oliveira et al., 2009; Meng & Ellis, 2015).

¹Anonymous Institution, Anonymous City, Anonymous Region, Anonymous Country. Correspondence to: Anonymous Author <anon.email@domain.com>.

Preliminary work. Under review by the International Conference on Machine Learning (ICML). Do not distribute.

Suboptimal plasmid architectures, plagued by incompatible regulatory elements or unstable repeat regions, frequently lead to metabolic burden, reduced expression efficiency, and manufacturing bottlenecks (Wu et al., 2016; Brophy & Voigt, 2011).

Current approaches to plasmid design rely heavily on tacit domain knowledge and piecemeal assembly of genetic parts. Designers must simultaneously optimize for competing objectives such as copy number, transcriptional output, and host viability while navigating the strict biophysical constraints of DNA folding and context dependent regulatory interactions (Deng et al., 2025; Fung et al., 2025).

To address these limitations, we introduce Plasmid-RL, a DNA language modeling framework for unconditional, end-to-end plasmid generation. Using PlasmidGPT as a testbed, Plasmid-RL adapts modern post-training techniques, including supervised fine-tuning (SFT) and reinforcement learning (RL), to the foundational genomic model (Shao et al., 2024a). This approach enables the model to internalize biological constraints and requirements, allowing it to reliably generate structurally valid and functionally coherent plasmid sequences. As demonstrated in our evaluation, Plasmid-RL achieves significantly higher quality control pass rates while maintaining acceptable sequence diversity, highlighting its potential to accelerate early stage design and minimize downstream verification efforts.

2. Background

2.1. DNA Language Models

Natural language processing and genomics have developed in parallel, often with algorithms developed for bioinformatics used in NLP and vice versa (Durbin et al., 1998). Natural language models pretrained on massive amounts of data have displayed emergent capabilities and remarkable utility by understanding the structure of language as a whole (Wei et al., 2022). These capabilities have vastly increased the utility of language models in a wide range of tasks, and are one of the primary reasons why large language model adoption has skyrocketed in the last few years. This has inspired the application of many similar techniques to genomic language models, resulting in models capable of impressive performance on biological tasks including vari-

055 ant prediction (Ji et al., 2021), transcription factor binding
056 site identification (Nguyen et al., 2023), and even whole-
057 genome generation (Nguyen et al., 2024).

058 Plasmid DNA has received relatively little attention com-
059 pared to other sequence types despite its importance in
060 biomanufacturing and wet lab research. OriGen (Martin-
061 son et al., 2025) introduces a generative model to produce
062 previously undiscovered origins of replication (ORIs) but
063 does not model whole sequences. PlasmidGPT (Shao et al.,
064 2024a) uses modern language modeling techniques to de-
065 velop a generative model for whole plasmid sequences, and
066 later work expands on this by synthesizing whole plasmids
067 generated using a fine tuned version of the PlasmidGPT
068 model (Cunningham et al., 2025). We use this as a base
069 model and apply post-training techniques to improve results
070 significantly.

072 2.2. Plasmid Design

073 Lab-designed plasmids are short circular DNA molecules
074 (typically 2–15 kb) that must contain multiple functional
075 components arranged in precise configurations. At mini-
076 mum, a viable plasmid requires: (i) an origin of replication
077 to enable autonomous replication, (ii) a selection marker
078 (e.g., antibiotic resistance gene) for identifying successfully
079 transformed cells, and (iii) a cloning site where genes of
080 interest can be inserted.

081 The search space of valid plasmids is massive due to com-
082 binatorial explosion across components. There are many
083 types of each component on the scale of hundreds to thou-
084 sand thousands per component, and additional regulatory ele-
085 ments (promoters, terminators, enhancers) and reporters may be
086 required depending on the application. Multiple instances
087 of certain components may be necessary, and the ordering
088 and spacing of these elements significantly impacts func-
089 tion. Beyond sheer combinatorics, designers must navigate
090 complex biological constraints including compatibility re-
091 quirements (specific ORIs only function in certain hosts),
092 physical stability issues (repeat regions can fold and bind to
093 each other), and other design challenges.

094 3. Methods

095 We follow an established method that starts with a base
096 model, fine-tunes it using supervised fine-tuning (SFT), and
097 then applies reinforcement learning (RL) to optimize for
098 specific attributes in the output.

100 3.1. Supervised Fine-Tuning

101 Supervised fine-tuning (SFT) was performed on a curated
102 corpus of *E. coli* plasmid sequences assembled from Plas-
103 midScope and Addgene. After deduplication and quality fil-
104 tering, approximately 15k circular plasmids (≤ 30 kb) were

105 retained, excluding linear entries, fragments, and incom-
106 plete records. Sequences were tokenized using the origi-
107 nal PlasmidGPT byte-pair DNA tokenizer. The pretrained
108 PlasmidGPT model was fine-tuned using an autoregressive
109 next-token prediction objective with gradient accumulation
110 and learning-rate warmup over three epochs.

3.2. Reinforcement Learning with GRPO

We implement a configurable reinforcement learning pipeline for plasmid design that uses Group Relative Policy Optimization (GRPO) (Shao et al., 2024b) with a domain-specific reward function described below. At each training iteration, the model generates a batch of candidate plasmids via autoregressive rollouts conditioned on short nucleotide prompts. Prompts are either stochastic (4–25 bp random seeds, excluding "ATG", used to promote rollout diversity) or structured (partial "cassette" seeds encoding canonical marker genes such as antibiotic-resistance or fluorescent reporters). Each candidate sequence is evaluated via our reward function, which captures structural plausibility, cassette organization, repeat content, and other biologically motivated constraints. GRPO is then applied to update the model parameters using these sequence-level rewards, enabling the policy to progressively shift toward generating plasmids with higher predicted validity.

3.3. Reward Function Design

The reward function scores each generated plasmid according to its structural plausibility and expected stability. It is composed of three conceptual components:

Functional annotation scoring: Lightweight annotations identify origins of replication, promoters, terminators, coding sequences (CDS), and selectable markers, which are then scored according to a configuration designed with subject matter expert (SME) input to reflect biologically reasonable quantities (e.g., exactly one origin of replication and at least one selectable marker). To encourage coherent gene cassettes, this component also includes a location-aware bonus for promoter → CDS → terminator arrangements that appear in the correct order and within a reasonable proximity window.

Length prior: A length prior favors plasmid sizes within typical experimental ranges (5–15 kb) preferred for plasmid construction.

Repeat penalty: A repeat penalty down-weights sequences containing long exact repeats that are associated with instability or recombination, specifically penalizing .1 reward for each repeat of length 50 bp or greater.

These terms are combined into a single scalar in [0, 1], yielding a fast and interpretable proxy for "plasmid-likeness" during reinforcement learning.

110
111
112
113
114
115
116
117
118
119
120
121
122
123
124
125
126
127
128
129
130
131
132
133
134
135
136
137
138
139
140
141
142
143
144
145
146
147
148
149
150
151
152
153
154
155
156
157
158
159
160
161
162
163
164

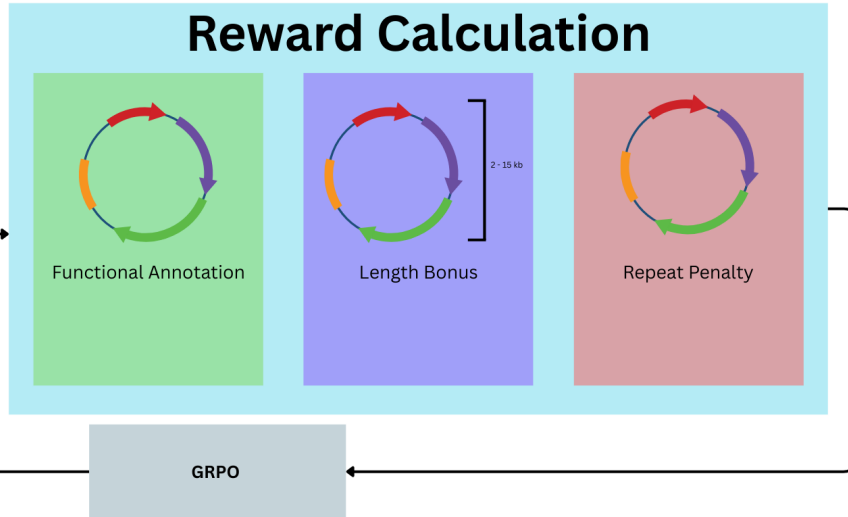


Figure 1. Overview of the Plasmid-RL training pipeline. Starting from the pretrained PlasmidGPT base model, we apply supervised fine-tuning on curated plasmid sequences, followed by reinforcement learning with Group Relative Policy Optimization using a biologically-motivated reward function that evaluates functional annotations, length constraints, and repeat content.

4. Experiments

4.1. Plasmid Quality Control and Uniqueness

We evaluate three model variants on held-out prompts not seen during training. For each model, we sampled 50 rollouts with two prompts: (i) a minimal prompt (single ATG codon) to test unconditional generation capability, and (ii) a structured prompt containing a complete GFP expression cassette to test the model’s ability to build around provided components. These prompts were deliberately excluded from the training corpus to ensure evaluation reflects generalization rather than memorization.

4.1.1. VALIDITY ASSESSMENT

In silico plasmid validity was assessed using a bioinformatics quality-control pipeline that leverages BLAST based tools, requiring exactly one origin of replication ($\geq 95\%$ identity and coverage), one or two antimicrobial resistance genes ($\geq 99\%$ identity and coverage), and no internal repeats longer than 50 bp (Altschul et al., 1990). This pipeline has been validated as a reliable proxy for experimental synthesis success (Cunningham et al., 2025). While we do not perform wet-lab validation in this work, our focus is on

establishing that RL post-training can successfully navigate the plasmid design space in silico, laying groundwork for future conditional generation systems where user-specified designs can be experimentally validated.

4.1.2. UNIQUENESS ASSESSMENT

To assess whether generated plasmids represent genuinely new designs rather than minor variants of existing constructs, we compute similarity to known sequences using the NCBI BLASTn API. Each generated plasmid is assigned to one of three categories based on identity and query-coverage thresholds: sequences with $\geq 99\%$ identity and $\geq 95\%$ coverage are classified as **Exists**; those with $\geq 95\%$ identity and $\geq 80\%$ coverage are **Similar**; and all others are classified as **Novel**.

This categorization is based on large scale data curation efforts such as PLSDB that use these thresholds of similarity to attempt to de-duplicate plasmids for not adding any additional value to a dataset (Galata et al., 2018).

4.1.3. DIVERSITY ASSESSMENT

To detect and prevent model collapse, we attempt to measure the diversity of the many samples of the model from the

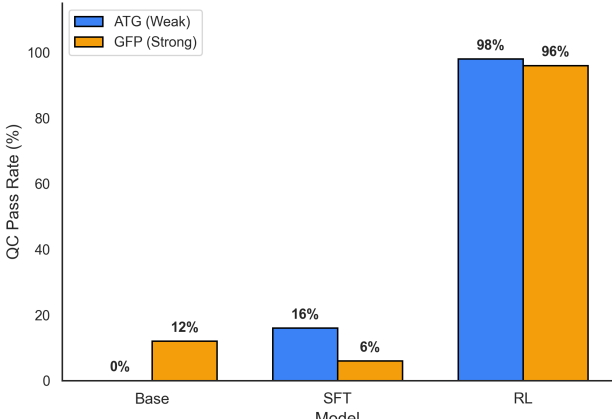


Figure 2. Summary of QC outcomes by prompt. Base model is only able to generate functional plasmids with a strong prompt. SFT allows the model to overcome this limitation on occasion but still often fails QC. Adding RL to the training process improves pass rate dramatically.

same prompt. Due to the lack of utility of traditional NLP metrics on this task, we use the mean Pairwise Jaccard distance of the 21-mers of each sequence. Diversity of a group of rollouts is calculated as follows:

$$D = 1 - \frac{1}{\binom{n}{2}} \sum_{i=1}^n \sum_{j=i+1}^n J(S_i, S_j)$$

where $J(S_i, S_j)$ is the Jaccard similarity between MinHash sketches of sequences i and j , and n is the number of sequences in the group.

The diversity metric (pairwise Jaccard distance) serves primarily as a model collapse detector rather than a biological validity measure. The RL model achieves 0.391 diversity compared to 0.926 for the base model, indicating that while the RL model concentrates probability mass on higher-quality regions of sequence space, it does not collapse to identical outputs. This is consistent with RL optimization finding conserved “successful motifs” (e.g., proven origins of replication, reliable resistance markers) while still maintaining sequence-level uniqueness.

4.1.4. RESULTS

Reinforcement learning substantially increases the probability of generating plasmids that pass our bioinformatics quality control (QC) pipeline, while supervised fine-tuning provides modest improvements. Figure 2 shows pass rates by prompt type, and Table 1 summarizes novelty and diversity metrics across models.

Table 1. Novelty and diversity metrics across model variants. RL achieves dramatically higher quality (97% pass rate) with reduced diversity in samples.

| MODEL | QC PASS RATE | % NOVEL | DIVERSITY |
|-------|--------------|---------|-----------|
| BASE | 6% | 95.5% | 0.926 |
| SFT | 11% | 100% | 0.886 |
| RL | 97% | 88% | 0.391 |

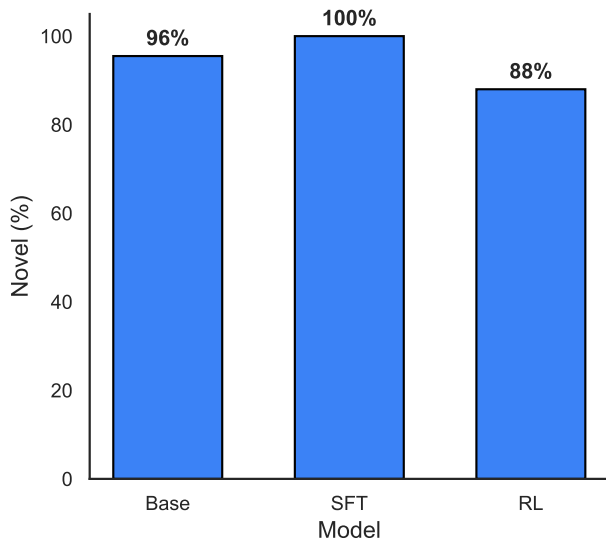


Figure 3. Summary of plasmid novelty as measured by comparison to NCBI database. SFT improves novelty of generated sequences from both base model and RL post-trained model.

When prompted with the weak ATG prompt, the base model never produces a valid plasmid (0%), whereas SFT increases the pass rate to 16%, and RL further increases it to 96%. A similar trend holds with the stronger GFP-cassette prompt: the base model achieves 12%, SFT drops to 4%, but the RL-optimized model reaches 76%.

Aggregated across strong and weak prompts, the overall QC pass rate rises from 6% with the base model to 11% with the SFT model and finally to 97% with the RL model, representing more than an order-of-magnitude improvement in validity relative to the pretrained baseline.

Importantly, this increase does not come from the RL models repeating previously known, high scoring sequences. Among passing sequences, the proportion classified as novel remains substantial for all models. Using our novelty thresholds, the RL model produces 88% novel plasmids among its QC-passing samples, compared to 95.5% for the base model. The SFT model generated 100% novel sequences. When normalized over all 100 rollouts per model, the RL

model produces 85.4% sequences that are both QC-valid and novel, compared to 11% for SFT and 6% for the base model.

Taken together, these results show that RL post-training not only dramatically improves biological plausibility but also preserves meaningful novelty relative to published plasmids. The model learns to satisfy constraints without collapsing to memorized or trivial constructs, suggesting that sequence-level RL can push generation toward realistic design regions while still exploring new areas of plasmid space.

4.2. Distribution Comparison

We compute several statistics known to be relevant to the performance of DNA from the raw sequences of both the generated plasmids and a small subset of real plasmids used for protein expression, genome editing, and other applications. See full details in the appendix. The distribution of the generated samples to each other and the real samples. We calculate the following summary statistics: sequence length distribution, GC content, longest open reading frame (ORF; calculated two ways), Jensen-Shannon divergence of the codon distribution, and Gibbs free energy (as calculated by ViennaRNA (Lorenz et al., 2011)).

Figure 4 shows that the RL post-trained model’s samples much more closely match the distributions of the real plasmids than the pretrained and supervised models, even when the metric is not directly encoded by the reward function.

Sequence length is directly encoded by the reward function, with optimal reward determined by a parameter sweep for training stability. GC content is not directly encoded, but regions selected for by the reward function likely have GC content distributed similarly to real plasmids. Despite generally making up a smaller percentage of the whole sequence, GC content is partially encoded by the reward function, as regions with higher GC content are more likely to be rewarded.

ORF length and codon distribution are not factored into the reward function directly. We calculate ORF length two ways: (1) maximum length of codons that are not stop codons on a single strand, and (2) longest stretch of non-stop codons after the presence of a start codon on either strand. These methods are disjoint from the method used to account for ORF in the reward function, which uses Prodigal (Hyatt et al., 2010) to predict and reward correctly placed ORFs. The ORF length, measured by either method, converges closely to the distribution of the real plasmids.

The same pattern holds for codon distribution and Gibbs free energy. While not accounted for in the reward function, the RL model learns to generate tokens with a much more similar codon distribution to real plasmids than the two models that have seen the correct distribution in the training data.

Table 2. Average log-probability on held-out continuation task. Higher values indicate better next-token prediction. RL shows unexpected improvement despite not being optimized for this task.

| MODEL | MEAN LOG-PROB | STD DEV |
|-------|---------------|---------|
| BASE | -12.449 | 6.144 |
| RL | -11.148 | 2.977 |

The similarity in the distribution of free energy measurements is particularly remarkable given that not only is free energy not optimized for directly, but no structural components are factored in at all excluding the weakly correlated repeat penalty originally included to solve recombination issues.

4.3. Held-Out Continuation

To evaluate how RL training affects nucleotide-level predictive performance, we measure how well each model can predict future bases given a real plasmid prefix. For each sequence, we provide the first 400 nucleotides as a prompt, have each model produce the next 100 nucleotides, and then compute the average log-probability of the true next 100 bases under each model. This allows us to compare the Base and RL models against real plasmids in terms of next-token prediction accuracy.

The RL model shows improved log-probability compared to the base model, with the standard deviation shrinking substantially from 6.144 to 2.977. This improvement is unexpected, as RL generally makes language models worse at next-token prediction tasks, a phenomenon known as the “alignment tax” (Lin et al., 2023).

4.4. Coding Sequence Surprisal Analysis

The reward function evaluates CDS regions using Prodigal rather than bioinformatics token-level approaches, reducing the risk of token-level information leakage. Because Prodigal predicts coding regions based only on generic statistical patterns and not on specific plasmid sequences, the reward signal is biologically grounded but distribution-agnostic. Interestingly, the RL-trained model achieves lower surprisal on real plasmids than the pretrained model, suggesting that the Prodigal-based reward sharpens the model’s understanding of natural plasmid structure.

5. Discussion

5.1. Diversity Trade-offs in Post-Training

One caveat to note is the decreased diversity of the post-trained model. This is a known effect of post-training but is especially noticeable in the domain of DNA sequence

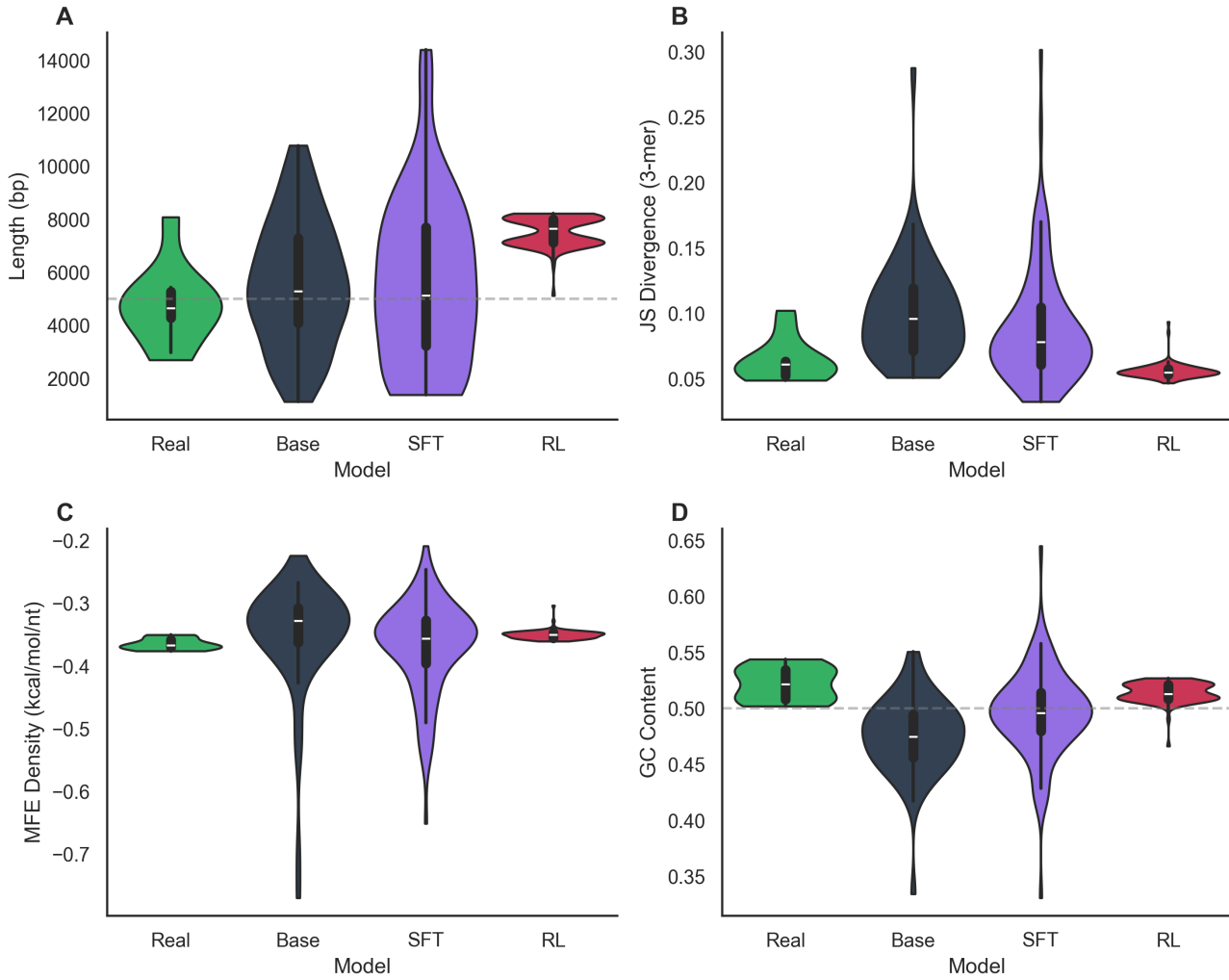


Figure 4. Distribution comparison across key biophysical metrics. The RL post-trained model (yellow) closely matches real plasmid distributions (blue) across sequence length, GC content, ORF length, codon usage (Jensen-Shannon divergence), and thermodynamic stability (Gibbs free energy), while the base model (green) and SFT model (orange) show substantial deviations. Notably, RL optimization produces realistic distributions even for metrics not explicitly encoded in the reward function.

generation. DNA in the context of this experiment can be thought of in two primary ways: (1) DNA that codes for a known region such as a promoter or an ORI, or (2) spacer DNA that exists primarily to contribute to structural stability.

While we observe a high degree of diversity in the sequences, there are some highly conserved regions that the post-trained model relies on to make the plasmid viable even more so than the base model. Conserved regions are necessary and common in nature, but the post-training process reduces the frequency with which some of the less common regions are used by the model. To make this concrete, when we sample the base model and the RL model 500 times each with the

weak ATG prompt and annotate all outputs, we see that the base model uses 10 unique ORIs while the RL model only uses 7.

This might explain some of the distribution patterns in Section 4.2, as the model finds a less diverse set of policies that work and explores less, leading to the shrunken variance and a more similar mean to the real plasmids. However, the experiments in Sections 4.3 and 4.4 suggest that the policy learned by the RL process is better aligned with natural plasmids, even on tasks involving next-token prediction and surprisal.

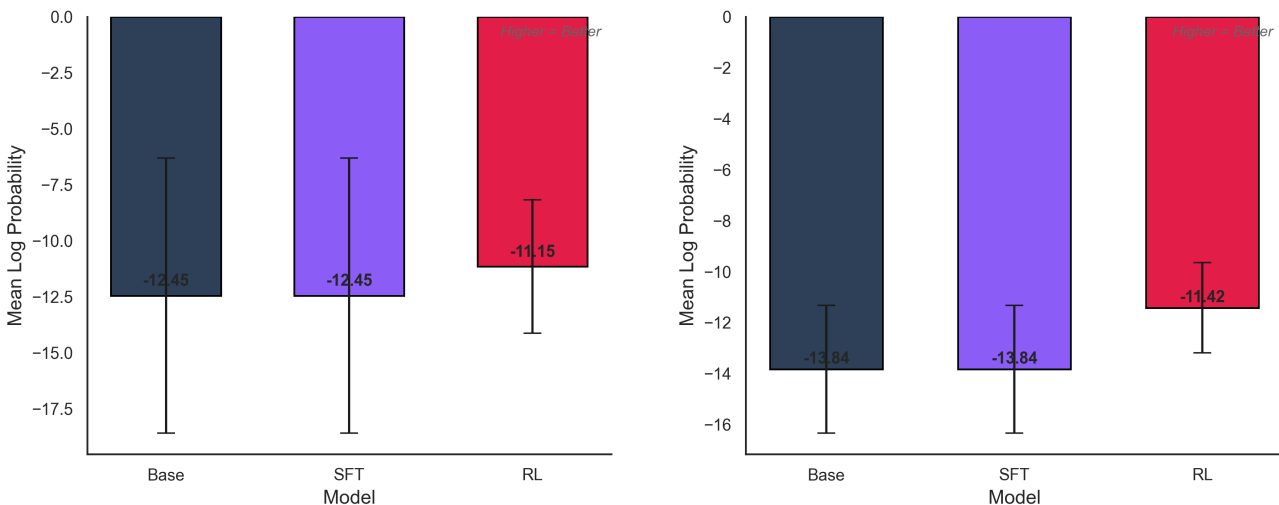


Figure 5. Held-out continuation performance across models. The RL model shows improved log-probability on real plasmid sequences, demonstrating better alignment with natural plasmid structure despite not being explicitly optimized for next-token prediction.

5.2. Limitations of Bioinformatic Evaluation

Our training and evaluation process is based almost entirely on bioinformatics, which depends on having a library of known regions. These libraries are naturally incomplete. Therefore, if our model ever generates a sequence that would work as an ORI, for example, but that sequence is missing from the library either by omission or because it has never been observed in nature before, the model will not receive a reward. This sharply limits how creative the model can be, and contrasts with other known examples of RL working well in domains such as natural language processing or protein design, where preference reward models or biophysical models are used, respectively.

5.3. Unexpected Improvement on Token-Level Tasks

Reinforcement learning typically makes language models worse on token-level tasks. This phenomenon, known as the “alignment tax,” makes sense intuitively: the model is optimized toward a policy to maximize a reward function and therefore away from the next-token prediction policy. Our model shows an interesting reversal of this trend.

One possible explanation uses the “steering vector” hypothesis as a way to understand how reinforcement learning interacts with the base model (Zou et al., 2023). This hypothesis states that the post-training process doesn’t give the model any new skills (more easily proven in NLP) but simply moves the latent space that the model decodes from

Figure 6. Coding sequence surprisal analysis. The RL model achieves lower surprisal on real plasmid coding sequences compared to the base and SFT models, indicating better capture of natural coding patterns despite using only Prodigal-based structural rewards.

to a more favorable region.

This offers a potential explanation as to why the reward function used was able to not only optimize plasmid validity as measured in silico (which is highly correlated with the reward function) but also optimize for thermodynamic stability and other characteristics that should be weakly correlated with the reward function. The RL process may have pushed the region of latent space toward a region of more valid plasmids in several aspects by being optimized for these bioinformatic features.

5.4. Emergent Properties and Evolutionary Analogies

The emergence of biologically realistic properties, reflexing those of real plasmids, while explicitly optimized mirros an evolutionary processes in that produce complex, correlated traits as byproducts of selecting for primary fitness criteria. Just as evolution optimizes for survival and reproduction while producing emergent phenomena like protein folding patterns and metabolic network architecture, our RL process optimizes for functional annotations while inducing realistic thermodynamic and sequence composition properties. This suggests that appropriately structured reward functions may capture sufficient biological constraints to guide models toward broadly realistic sequence space regions.

385 **5.5. Future Work: Conditional Generation**

386 This work further supports the ongoing hypothesis that modern language modeling techniques can be applied to DNA
387 language models in a similar fashion to how they have been
388 applied to natural language in the past. The real utility of
389 natural language models came from instruction tuning them
390 to respond to questions and follow directions. This work
391 shows that post-training techniques can be applied to DNA
392 language models to achieve similar results.

393 We hope to build out a dataset designed for conditional
394 generation where the user can prompt the model with the
395 specifics of the plasmid they want, and the model will de-
396 velop it from there. This would enable practical use cases
397 such as “design a plasmid for expressing protein X in E. coli
398 with high copy number” or “create a mammalian expression
399 vector with constitutive GFP expression.”

400 In addition to being far more practical than unconditional
401 generation, the conditioning will promote more diversity of
402 sample and make evaluation of the model’s performance on
403 the task of plasmid design much more understandable.

404 **6. Conclusion**

405 We have introduced Plasmid-RL, a reinforcement learning-
406 enhanced DNA language model framework for plasmid
407 design that achieves substantial improvements in both val-
408 idity and novelty compared to pretrained baselines. Our
409 model generates structurally valid plasmids at a 97% rate
410 (compared to 6% for the base model) while maintaining
411 88% novelty among valid sequences. Remarkably, the RL
412 training not only optimizes for explicitly rewarded features
413 but also induces emergent properties such as realistic ther-
414 modynamic stability and codon usage patterns.

415 These results demonstrate that modern post-training tech-
416 niques from natural language processing can be effectively
417 adapted to biological sequence design, opening new avenues
418 for accelerating synthetic biology workflows. The unex-
419 pected improvement in next-token prediction suggests
420 that RL may be steering the model toward more biologi-
421 cally coherent regions of sequence space rather than simply
422 memorizing solutions.

423 Future work will extend this framework to conditional gen-
424 eration, enabling user-directed plasmid design (e.g., “express
425 protein X in E. coli with high copy number”), at which
426 point experimental validation of model-generated sequences
427 will be critical. Additionally, we aim to apply these tech-
428 niques to other models and biological sequence classes,
429 further demonstrating the generality of RL post-training for
430 biomolecular design.

431 **Impact Statement**

432 This paper presents work whose goal is to advance the field
433 of computational biology and machine learning for biological
434 sequence design. The ability to generate novel, valid
435 plasmid sequences could accelerate research in synthetic
436 biology, biomanufacturing, and therapeutic development.
437 While the immediate applications are primarily beneficial
438 for scientific research, we acknowledge the dual-use nature
439 of synthetic biology tools. The methods described here
440 are limited to generating plasmid sequences based on pat-
441 terns in existing databases and do not enable the design of
442 harmful organisms without substantial additional effort and
443 expertise. We believe the benefits to research efficiency and
444 accessibility outweigh the potential risks, particularly given
445 existing biosafety regulations and oversight mechanisms in
446 synthetic biology research.

447 **Code Availability**

448 Code for model training and evaluation will be released
449 upon publication. Training data is derived from Plasmid-
450 Scope and Addgene databases, available under their respec-
451 tive licenses.

452 **Acknowledgements**

453 We thank the PlasmidGPT team for providing the base
454 model and the computational biology community for making
455 plasmid sequence databases publicly available.

440 A. Training Configuration Details

441 A.1. Supervised Fine-Tuning Hyperparameters

- 442 • **Batch size:** 1
- 443 • **Learning rate:** 5×10^{-5} with 500 warmup steps
- 444 • **Optimizer:** AdamW
- 445 • **Epochs:** 3
- 446 • **Gradient accumulation steps:** 8
- 447 • **Hardware:** [single/multi] NVIDIA L4 GPU(s)

448 A.2. Reinforcement Learning (GRPO) 449 Hyperparameters

- 450 • **Rollout batch size:** 50
- 451 • **Policy learning rate:** 3.55×10^{-5} (found via hyperparameter sweep)
- 452 • **GRPO group size:** 16
- 453 • **Training steps:** Varies between 1000-2500 (scheduled for 2500 but rarely reached due to early convergence)
- 454 • **Convergence criteria:** Reward plateau or dip indicating collapse
- 455 • **Prompt types:** Random 4–25bp seeds (excluding ATG) and structured cassette seeds
- 456 • **Total training time:** ~10–20 hours on NVIDIA L4 GPU

457 A.3. Reward Function Configuration

- 458 • **Origin of replication (exactly 1):** Weight = 1.0
- 459 • **Selectable markers (≥ 1):** Weight = 1.5
- 460 • **Promoter→CDS→terminator bonus:** Weight = 1.5
- 461 • **Length prior (2–15kb):** Weight = 0.6, linear with maximum reward at 5kb and minimum at 15kb, zero reward beyond 15kb
- 462 • **Repeat penalty (>50bp):** -0.1 from total reward for each repeat > 50bp

463 A.4. Reference Plasmids for Distribution Comparison

464 The following common laboratory plasmids were used for distribution comparison and benchmarking analyses in Section 4.2:

| Plasmid | Size (bp) | Description |
|-------------------------------------|-----------|--------------------------------|
| pUC19 (Yanisch-Perron et al., 1985) | 2,686 | High-copy cloning vector |
| pBluescript (Short et al., 1988) | 2,961 | Cloning vector |
| pBR322 (Bolivar et al., 1977) | 4,361 | Classic cloning vector |
| pACYC184 (Chang & Cohen, 1978) | 4,245 | Low-copy vector |
| pBAD24 (Guzman et al., 1994) | 4,542 | Arabinose-inducible expression |
| pEGFP (Clontech Laboratories, 1999) | 4,733 | GFP expression vector |
| pGEX-4T-1 (GE Healthcare, 2000) | 4,969 | GST fusion expression |
| pET-28a (Novagen, 2005) | 5,369 | T7 expression vector |
| pcDNA3 (Kaufman et al., 1991) | 5,428 | Mammalian expression |
| px330 (Cong et al., 2013) | 8,074 | CRISPR/Cas9 vector |

465 These plasmids represent widely-used vectors spanning diverse applications (cloning, protein expression, mammalian transfection, genome editing) and size ranges (2.7–8.1 kb), providing a representative benchmark for evaluating the biological realism of generated sequences.

466 References

- 467 Altschul, S. F., Gish, W., Miller, W., Myers, E. W., and Lipman, D. J. Basic local alignment search tool. *Journal of Molecular Biology*, 215(3):403–410, 1990.
- 468 Bolivar, F., Rodriguez, R. L., Greene, P. J., Betlach, M. C., Heyneker, H. L., Boyer, H. W., Crosa, J. H., and Falkow, S. Construction and characterization of new cloning vehicles. II. A multipurpose cloning system. *Gene*, 2(2): 95–113, 1977.
- 469 Brophy, J. A. and Voigt, C. A. Plasmid design for tunable gene expression in bacteria. *Methods in Enzymology*, 497: 371–388, 2011.
- 470 Chang, A. C. and Cohen, S. N. Construction and characterization of new cloning vehicles. V. Mobility and coding functions of pbr322 and pbr325 'derived' plasmids. *Journal of Bacteriology*, 134(3):1141–1156, 1978.
- 471 Clontech Laboratories. pEGFP vector information. Product Manual, 1999. Catalog #6077-1.
- 472 Cong, L., Ran, F. A., Cox, D., Lin, S., Barretto, R., Habib, N., Hsu, P. D., Wu, X., Jiang, W., Marraffini, L. A., et al. Multiplex genome engineering using CRISPR/Cas systems. *Science*, 339(6121):819–823, 2013.
- 473 Cunningham, A. G., Dekker, L., Shcherbakova, A., and Barnes, C. P. Generative design and construction of functional plasmids with a dna language model. *bioRxiv*, 2025. doi: 10.1101/2025.12.06.692736. URL <https://www.biorxiv.org/content/early/2025/12/07/2025.12.06.692736>.
- 474 Deng, Y., Maurais, H. E., Etheridge, K., and Sarapeshkar, R. Gene syntaxes modulate gene expression and circuit behavior on plasmids. *Journal of Biological Engineering*, 19(1):25, 2025. doi: 10.1101/2025.12.06.692736.
- 475

- 495 s13036-025-00493-0. URL <https://doi.org/10.1186/s13036-025-00493-0>.
- 496
- 497 Durbin, R., Eddy, S. R., Krogh, A., and Mitchison, G. *Biological Sequence Analysis: Probabilistic Models of Proteins and Nucleic Acids*. Cambridge University Press, 1998. ISBN 9780521629713.
- 498
- 499
- 500
- 501
- 502 Fung, V., Tiwade, P. B., and Fenton, O. S. Clonefast: A simple plasmid design and construction guide for labs venturing into synthetic biology. *STAR Protocols*, 6(3):104025, 2025. ISSN 2666-1667. doi: <https://doi.org/10.1016/j.xpro.2025.104025>. URL <https://www.sciencedirect.com/science/article/pii/S2666166725004319>.
- 503
- 504
- 505
- 506
- 507
- 508
- 509
- 510 Galata, V., Fehlmann, T., Backes, C., and Keller, A. Plsdb: a resource of complete bacterial plasmids. *Nucleic Acids Research*, 47(D1):D195–D202, 10 2018. ISSN 0305-1048. doi: 10.1093/nar/gky1050. URL <https://doi.org/10.1093/nar/gky1050>.
- 511
- 512
- 513
- 514
- 515
- 516 GE Healthcare. pGEX vectors. Product Manual, 2000. GST Gene Fusion System.
- 517
- 518
- 519 Guzman, L.-M., Belin, D., Carson, M. J., and Beckwith, J. Making transcriptional silencers work in Escherichia coli. *Molecular Microbiology*, 13(4):655–662, 1994.
- 520
- 521
- 522
- 523 Hyatt, D., Chen, G.-L., LoCascio, P. F., Land, M. L., Larimer, F. W., and Hauser, L. J. Prodigal: prokaryotic gene recognition and translation initiation site identification. *BMC Bioinformatics*, 11(1):1–11, 2010. doi: 10.1186/1471-2105-11-119.
- 524
- 525
- 526
- 527
- 528
- 529 Ji, Y., Zhou, Z., Liu, H., and Davuluri, R. V. DNABERT: pre-trained bidirectional encoder representations from transformers model for DNA-language in genome. *Bioinformatics*, 37(15):2112–2120, 2021.
- 530
- 531
- 532
- 533
- 534 Kaufman, R. J., Davies, M. V., Pathak, V. K., and Hershey, J. W. A mammalian expression vector for the expression of complete open reading frames. *Nucleic Acids Research*, 19(16):4485–4490, 1991.
- 535
- 536
- 537
- 538 Kutzler, M. A. and Weiner, D. B. Plasmid DNA vaccines: an overview. *Vaccine*, 26:S59–S75, 2008.
- 539
- 540
- 541 Lederberg, J. Cell genetics and hereditary symbiosis. *Physiological Reviews*, 32(4):403–430, 1952. Seminal paper defining the term “plasmid”.
- 542
- 543
- 544 Lin, Y., Dong, H., Wang, H., Zhang, J., Liu, J., Pi, R., Pan, R., Zhang, H., Hu, W., Zhao, H., et al. Mitigating the alignment tax of RLHF. *arXiv preprint arXiv:2309.06256*, 2023.
- 545
- 546
- 547
- 548
- 549 Lorenz, R., Bernhart, S. H., Höner zu Siederdissen, C., Tafer, H., Flamm, C., Stadler, P. F., and Hofacker, I. L. ViennaRNA package 2.0. *Algorithms for Molecular Biology*, 6 (1):26, 2011.
- 550
- 551 Martinson, J. N. V. et al. Generating functional plasmid origins with OriGen. *Nucleic Acids Research*, 53(22):gkaf1198, 2025. doi: 10.1093/nar/gkaf1198.
- 552
- 553 Meng, F. and Ellis, T. Challenges in rational design of synthetic promoters. *New Biotechnology*, 32(3):337–344, 2015.
- 554
- 555 Nguyen, E., Poli, M., Faizi, M., Thomas, A., Birch-Sykes, C., Wornow, M., Patel, A., Rabideau, C., Massaroli, S., Bengio, Y., et al. HyenaDNA: Long-range genomic sequence modeling at single nucleotide resolution. *arXiv preprint arXiv:2306.15794*, 2023.
- 556
- 557 Nguyen, E., Poli, M., Durrant, M. G., Kang, B., Katrekar, D., Li, D. B., Bartie, A., Thomas, A. W., King, S. H., Bifulco, G., et al. Sequence modeling and design from molecular to genome scale with Evo. *bioRxiv*, 2024. doi: 10.1101/2024.02.27.582234.
- 558
- 559 Novagen. pET system manual. Product Manual, 11th Edition, 2005. TB055.
- 560
- 561 Oliveira, P. H., Prather, K. L., Prazeres, D. M., and Monteiro, G. A. Structural instability of plasmid biopharmaceuticals: challenges and implications. *Trends in Biotechnology*, 27(9):503–511, 2009.
- 562
- 563 Prather, K. J., Sagar, S., Murphy, J., and Chartrain, M. Industrial scale production of plasmid DNA for vaccine and gene therapy: plasmid design, production, and purification. *Enzyme and Microbial Technology*, 33(7):865–883, 2003.
- 564
- 565 Shao, L. et al. PlasmidGPT: a generative framework for plasmid design and annotation. *bioRxiv*, 2024a. doi: 10.1101/2024.09.30.615762. Preprint.
- 566
- 567 Shao, Z., Wang, P., Zhu, Q., Xu, R., Song, J., Zhang, M., Li, Y. K., Wu, Y., and Guo, D. DeepSeekMath: Pushing the limits of mathematical reasoning in open language models. *arXiv preprint arXiv:2402.03300*, 2024b.
- 568
- 569 Short, J., Fernandez, J., Sorge, J., and Huse, W. Bluescript: a high copy number Escherichia coli plasmid vector. *Nucleic Acids Research*, 16(15):7583–7600, 1988.
- 570
- 571 Wei, J., Tay, Y., Bommasani, R., Raffel, C., Zoph, B., Borgeaud, S., Yogatama, D., Bosma, M., Zhou, D., Metzler, D., Chi, E. H., Hashimoto, T., Vinyals, O., Liang, P., Dean, J., and Fedus, W. Emergent abilities of large language models, 2022. URL <https://arxiv.org/abs/2206.07682>.

550 Wu, G., Yan, Q., Jones, J. A., Tang, Y. J., Fong, S. S.,
551 and Koffas, M. A. Metabolic burden: cornerstones in
552 synthetic biology and metabolic engineering applications.
553 *Trends in Biotechnology*, 34(8):652–664, 2016.

554 Yanisch-Perron, C., Vieira, J., and Messing, J. New M13
555 vectors for cloning. *Gene*, 33(1):103–119, 1985.

557 Zou, A., Phan, L., Chen, S., Campbell, J., Guo, P., Ren, R.,
558 Pan, A., Yin, X., Mazeika, M., Dombrowski, A.-K., et al.
559 Representation engineering: A top-down approach to AI
560 transparency. *arXiv preprint arXiv:2310.01405*, 2023.

561

562

563

564

565

566

567

568

569

570

571

572

573

574

575

576

577

578

579

580

581

582

583

584

585

586

587

588

589

590

591

592

593

594

595

596

597

598

599

600

601

602

603

604